Pergamon

Journal of Structural Geology, Vol. 19, No. 7, pp. 1011 to 1014, 1997

PII: S0191-8141(97)00027-8
0191-8141/97 $17.00 + 0.00

Brevia

SHORT NOTES

Strains within thrust-wrench zones

OLIVIER MERLE

Université Blaise Pascal, Département des Sciences de la Terre, 5 rue Kessler, 63038 Clermont-Ferrand cedex, France

and

DENIS GAPAIS

Géosciences Rennes, UPR 4661 CNRS, Université de Rennes 1, 35042 Rennes cedex, France

(*Received* 10 *September* 1996; *accepted in revised form* 28 *February* 1997)

Abstract—Finite strains resulting from combined wrenching and thrusting (or extension) are expected to be rather common in many tectonic contexts, for example during oblique convergence. In this brevia, we examine finite strains resulting from such deformations using a numerical simulation. In our simulation, oblique convergence environments produce flattening or plane strains, whereas oblique divergence environments yield constrictional or plane strains. Different combinations of wrenching and thrusting can yield principal strain directions with comparable orientations. Results emphasize that finite strain analysis alone may be of rather limited interest, even in relatively simple kinematic environments. © 1997 Elsevier Science Ltd.

INTRODUCTION

Most tectonic environments involve oblique displacements with respect to major crustal discontinuities. When studying oblique convergence in Caledonian Spitzbergen, Harland (1971) was the first to introduce the term transpression to describe this process on the scale of tectonic plates.

Strain patterns associated with oblique convergence have been described by different authors using numerical models involving combinations of two simple shears, pure wrenching and pure thrusting, along inclined shearing planes (e.g. Brun and Burg, 1982; Ellis and Watkinson, 1987). These studies have shown the relationship between convergence angle and stretch direction, which may occur, for instance, along a subducting plate during oblique convergence.

Other authors have studied transpression using numerical combinations of simple shear parallel to the strike and pure shear across a ductile shear zone (e.g. Sanderson and Marchini, 1984; Fossen and Tikoff, 1993; Robin and Cruden, 1994; Tikoff and Teyssier, 1994; Jones and Tanner, 1995). These studies made it possible to understand the strain arising from the simultaneous combination of pure shear and simple shear, the pure shear component corresponding to horizontal shortening at right angles to the along-strike simple shear component. This may correspond to the strain encountered in deep parts of major ductile shear zones accommodating oblique convergence.

However, oblique convergence also can result in pervasive deformations resulting from more general combinations of wrenching and thrusting. This is, for example, expected in flower structures where the major shear zone is bounded by convex-upward faults, that is thrusts that steepen inward and downward. In this brevia article, we examine how penetrative strains may vary across such deformation zones. Compared with previous studies, our numerical model does not involve a pure shear component perpendicular to the strike of the transcurrent shear zone, but combines a component of wrenching γ_w along a vertical plane with an oblique component of thrusting γ_T (Fig. 1). Critical parameters are the inclination θ of the thrusting plane and the angle α between thrusting and wrenching directions. Our results emphasize that finite strain analysis must be used with caution and may often yield very limited kinematic conclusions.

THEORY

The two deformation matrices for three-dimensional wrenching (D_W) and thrusting (D_T) deformations (see coordinate system on Fig. 1) are as follows:

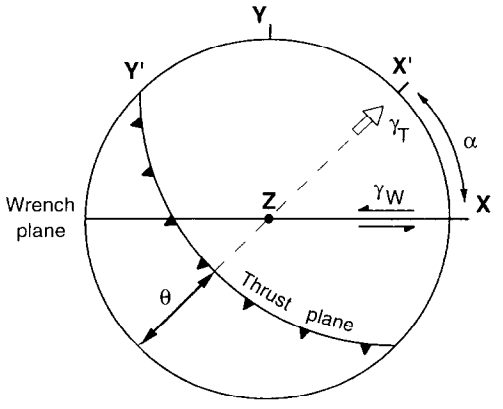

Fig. 1. Lower-hemisphere stereogram showing coordinate axes (x, y and z) of the numerical model. Thrusting component (γ_T) is oriented at α degrees with respect to the E–W wrenching component (γ_W), and inclined at $\theta°$ to the horizontal.

$$D_W = \begin{vmatrix} 1 & \gamma_W & 0 \\ 0 & 1 & 0 \\ 0 & 0 & 1 \end{vmatrix}, D_T = \begin{vmatrix} 1 & 0 & \gamma_T \\ 0 & 1 & 0 \\ 0 & 0 & 1 \end{vmatrix}. \quad (1)$$

These two deformation matrices, more specifically the D_T part, only apply when $\alpha = \theta = 0$. Positive or negative γ_W yields dextral or sinistral sense of wrenching, respectively. In our model coordinates, the wrenching component is E–W and sinistral, compatible with the thrusting direction, which lies in the NE–SW quadrant (Fig. 1). In this coordinate system, dextral wrenching combined with a negative γ_T component corresponds to an oblique divergence deformation.

The two rotation matrices associated with the angle α between the two directions of simple shear and the inclination θ of the thrusting plane are as follows (Fig. 1):

$$R_\alpha = \begin{vmatrix} \cos\alpha & \sin\alpha & 0 \\ -\sin\alpha & \cos\alpha & 0 \\ 0 & 0 & 1 \end{vmatrix}, R_\theta = \begin{vmatrix} \cos\theta & 0 & \sin\theta \\ 0 & 1 & 0 \\ -\sin\theta & 0 & \cos\theta \end{vmatrix}. \quad (2)$$

The total strain is then given by the following deformation matrix:

$$D_{WT} = R_\alpha^{-1}.R_\theta^{-1}.D_T.R_\theta.R_\alpha.D_W. \quad (3)$$

This total strain corresponds to a wrenching deformation in the x direction, followed by a thrusting deformation in the x' direction which can be inclined at $\theta°$ to the horizontal (Fig. 1). To combine the wrenching and thrusting deformations simultaneously, the deformation matrix proposed by Tikoff and Fossen (1993) could not be used, as it requires the two shear planes to be mutually orthogonal, a condition that is not fulfilled in our deformational process. A simultaneous combination can be obtained from the strain-rate tensor as proposed by Ramberg (1975a,b). This rigorous method has already been used to compute strain patterns in particular kinematic settings [for further details, see Coward and Kim (1981) and Merle (1989)]. Alternatively, an approximate solution may be obtained by multiplying successive small increments of wrenching and thrusting. This approach becomes identical to a continuous integration, provided that strain increments are sufficiently small (Ramberg, 1975a,b). We have used this step-by-step procedure, with shear increments of 0.01 and a constant γ_W/γ_T ratio, equal to 1. Strain then can be computed from the symmetrical Finger tensor ($D_{WT}D_{WT}^t$) (Malvern, 1969), which has eigenvalues equal to the principal quadratic elongation $(1+e_i)^2$ and eigenvectors parallel to the principal strain axes (see De Paor, 1983).

RESULTS

Shape of strain ellipsoid

The computation of the Flinn parameter [$k = (\lambda_1/\lambda_2 - 1)/(\lambda_2/\lambda_3 - 1)$, $\lambda_i = 1 + e_i$] makes it possible to predict the rock fabric that is expected to result from our deformation process. Figure 2 shows contours of k values as a function of α and θ.

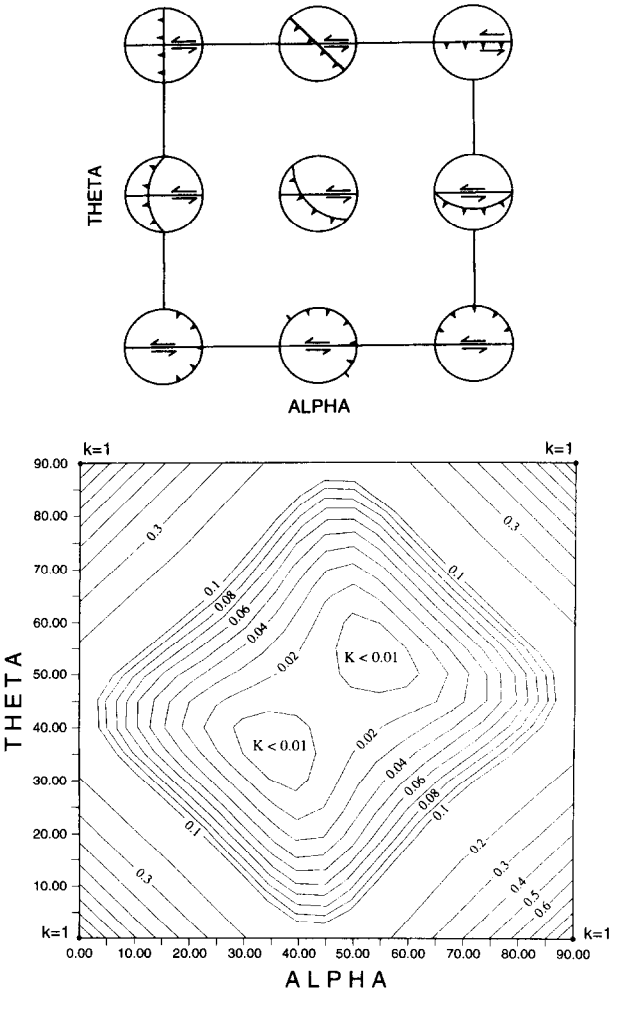

Fig. 2. Contours of values of Flinn parameter (k) as a function of α and θ. The top sketch shows the relative attitudes of thrust and wrench components (lower hemisphere stereogram) for the nine singular points of the diagramm.

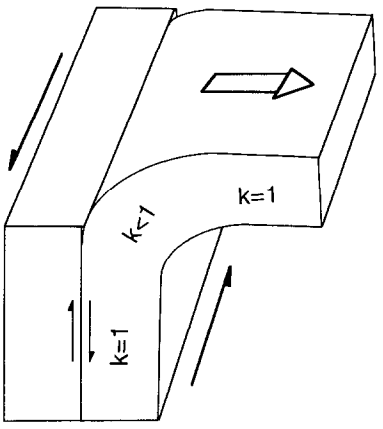

Fig. 3. Schematic representation of a curved thrust-wrench shear zone parallel to the strike of a positive flower structure. Strain is of flattening type ($k<1$), except along the deepest vertical termination ($\alpha=90$ and $\theta=90$) and along the flat-lying external termination ($\alpha=90$ and $\theta=0$) where plane strain occurs ($k=1$).

Four singular points are characterized by strain plane ($k=1$). They correspond to the four combinations of angle α equal to 0 or 90, with angle θ equal to 0 and 90. Two of them are unlikely to occur in nature ($\alpha=\theta=0$, and $\alpha=0$ with $\theta=90$). The two other situations might occur, for instance, in end-member situations encountered in a curved thrust-wrench shear zone parallel to the strike of a positive flower structure, within its deepest vertical parts ($\alpha=90$ and $\theta=90$) and its external flat-lying terminations ($\alpha=90$ and $\theta=0$) (Fig. 3).

For all other combinations of α and θ angles, the strain is of flattening type ($k<1$) (Fig. 2). The lowest k values occur for α and θ angles ranging between 30 and 60°. More remarkable is the symmetry of the diagram with respect to both upper left-lower right and upper right-lower left diagonals (Fig. 2). This emphasizes that different deformations, involving various combinations of α and θ angles, can yield finite strain ellipsoids with similar shapes.

It is worthwhile noting that the strain diagram obtained for oblique divergence environments ($\gamma_W>0$ and $\gamma_T<0$) is the mirror image of that shown on Fig. 2 with respect to plane strain conditions: except for the four singular combinations of α and θ that result in plane-strain, oblique divergence deformations yield strain ellipsoids of constriction type, highest k values being observed for α and θ angles ranging between 30 and 60°.

Attitude of principal strain axes

Figure 4 shows the attitudes of principal strains for four representative examples of E–W sinistral strike–slip combined with thrusting on a 30° dipping plane, along a direction ranging between NE–SW and N–S. Such conditions are likely to occur in a sinistral oblique convergence environment. For each stereogram, five stages of increasing strain are shown. These examples emphasize that comparable attitudes of both schistosity and stretching lineation can be observed for different types of combination of wrenching and thrusting. More generally, no simple discriminatory relationships were observed among the dip θ of the thrusting component, the angle α between thrusting and wrenching directions, and the resulting attitude of principal strain axes.

The strike of the principal flattening plane (schistosity plane $\lambda_1\lambda_2$) varies between NW–SE and E–W with increasing strain, irrespective of the relative attitudes of thrusting and wrenching components (Fig. 4). The dip of the principal flattening plane varies according to both relative attitudes of thrusting and wrenching components and strain intensity. It turns out that different combinations of thrusting and wrenching components can yield principal flattening planes with similar strike and dip. Similar conclusions can be drawn from the orientation of the principal stretching direction λ_1 (see Fig. 4).

However, it should be noted that the shape of the strain ellipsoid (Flinn parameter k) is different in each of the four examples shown on Fig. 4. Although strain ratios potentially could distinguish between these cases, one could question whether strain measurements in the field are accurate enough to discriminate clearly among them. Conversely, different combinations of alpha and theta angles with identical k values often yield similar attitudes of principal strain directions.

CONCLUDING REMARKS

The above numerical combinations of wrenching and thrusting allow us to draw the following conclusions:

(1) Penetrative strains resulting from combined wrenching and thrusting are of a flattening to plane-strain type. However, one must keep in mind that variable proportions of wrenching and thrusting components are expected to occur in zones of oblique convergence, a feature that has not been considered in the present paper. Nevertheless, natural examples suggest that flattening strains are common within thrust-wrench deformation zones. For example, Cobbold *et al.* (1991) have argued for widespread flattening strains within the Hercynian arcuate belt of the Sierras Australes (Argentina), where ductile deformation results from combinations of wrenching and thrusting in various proportions.

(2) Conversely, constriction or plane-strain is expected to occur in oblique divergent environments.

(3) Ductile deformation involving combinations of wrenching and thrusting (or extension) with different angular relationships between the two simple shears can yield schistosities and stretching lineations with comparable or similar attitudes. The same is observed for strain ellipsoid shapes.

(4) The above features emphasize that finite strain analysis is a limited tool to infer bulk kinematics, even where the deformation history is rather simple. Relevant information on kinematics, however, may be obtained in

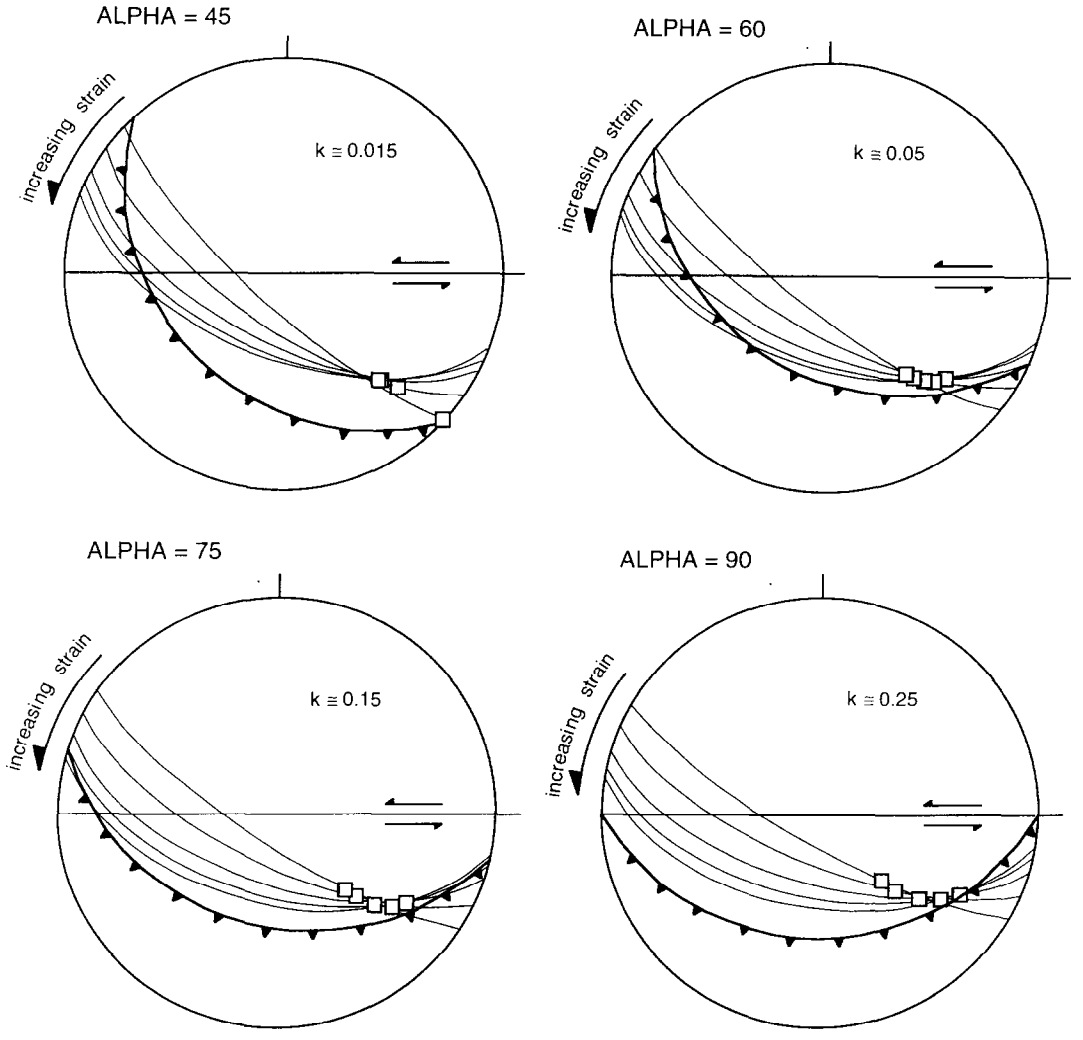

Fig. 4. Lower-hemisphere stereograms showing principal flattening planes (light great circles) and principal stretch directions (squares) resulting from combined E–W sinistral wrenching (arrows) and thrusting along a 30° dipping plane ($\theta = 30°$, heavy large circles) for four values (45°, 60°, 75° and 90°) of alpha (angle between thrusting and wrenching directions). k values are indicated in each stereogram.

situations in which analyses of infinitesimal strain indicators and shear criteria help to estimate the attitude of the two principal shear planes (i.e. α and θ).

Acknowledgements—We would like to thank A. Cruden, P. J. Hudleston and B. Tikoff for their kind reviews of the manuscript.

REFERENCES

Brun, J. P. and Burg, J. P. (1982) Combined thrusting and wrenching in the Ibero-Armorican arc: a corner effect during continental collision. *Earth and Planetary Science Letters* **61**, 319–332.

Cobbold, P. R., Gapais, D. and Rossello, E. A. (1991) Partitioning of transpressive motions within a sigmoidal foldbelt: the Variscan Sierras Australes, Argentina. *Journal of Structural Geology* **13**, 743–758.

Coward, M. P. and Kim, J. H. (1981) Strain within thrust sheets. In *Thrust and Nappe Tectonics. Geological Society Special Publication*, Vol. 9, pp. 275-292.

De Paor, D. G. (1983) Orthographic analysis of geological structures I. Deformation theory. *Journal of Structural Geology* **5**, 255–277.

Ellis, M. and Watkinson, J. (1987) Orogen-parallel extension and oblique tectonics: the relation between stretching lineations and relative plate motions. *Geology* **15**, 1022–1026.

Fossen, H. and Tikoff, B. (1993) The deformation matrix for simultaneous pure shear, simple shear, and volume change, and its application to transpression/transtension tectonics. *Journal of Structural Geology* **15**, 413–422.

Harland, W. B. (1971) Tectonic transpression in Caledonian Spitzbergen. *Geological Magazine* **108**, 27–42.

Jones, R. R. and Tanner, P. W. (1995) Strain partitioning in transpression zones. *Journal of Structural Geology* **17**, 793–802.

Malvern, L. E. (1969) *Introduction to the Mechanics of a Continuous Medium*. Prentice-Hall, Englewood Cliffs, NJ, 713 pp.

Merle, O. (1989) Strain pattern within spreading nappes. *Tectonophysics* **165**, 57–71.

Ramberg, H. (1975) Particle paths, displacement and progressive strain applicable to rocks. *Tectonophysics* **28**, 1–37.

Ramberg, H. (1975) Superposition of homogeneous strain and progressive deformation in rocks. *Bulletin of the Geological Institute of the University of Uppsala* **6**, 35–67.

Robin, P.-Y. F. and Cruden, A. R. (1994) Strain and vorticity patterns in ideally ductile transpression zones. *Journal of Structural Geology* **16**, 447–466.

Sanderson, D. J. and Marchini, W. R. D. (1984) Transpression. *Journal of Structural Geology* **6**, 449–458.

Tikoff, B. and Fossen, H. (1993) Simultaneous pure and simple shear: the unifying deformation matrix. *Tectonophysics* **217**, 267–283.

Tikoff, B. and Teyssier, C. (1994) Strain modelling of displacement-field partitioning in transpressional orogens. *Journal of Structural Geology* **16**, 1575–1588.